Chitosan-based microparticles for immobilization of TiO2 nanoparticles and their application for photodegradation of textile dyes

Skoric, Marija Lucic; Terzic, Ivan; Milosavljevic, Nedeljko; Radetic, Maja; Saponjic, Zoran; Radoicic, Marija; Krusic, Melina Kalagasidis

Published in:
European Polymer Journal

DOI:
10.1016/j.eurpolymj.2016.06.026

European Polymer Journal 82 (2016) 57–70

Contents lists available at ScienceDirect

European Polymer Journal

journal homepage: www.elsevier.com/locate/europolj

Macromolecular Nanotechnology

Chitosan-based microparticles for immobilization of TiO_2 nanoparticles and their application for photodegradation of textile dyes

Marija Lučić Škorić [a], Ivan Terzić [b], Nedeljko Milosavljević [a], Maja Radetić [c], Zoran Šaponjić [d], Marija Radoičić [d], Melina Kalagasidis Krušić [a,*]

[a] University of Belgrade, Department of Organic Chemical Technology, Faculty of Technology and Metallurgy, Karnegijeva 4, 11120 Belgrade, Serbia
[b] Department of Polymer Chemistry, Zernike Institute for Advanced Materials, University of Groningen, Nijenborgh 4, 9747 AG Groningen, The Netherlands
[c] University of Belgrade, Textile Engineering Department, Faculty of Technology and Metallurgy, Karnegijeva 4, 11120 Belgrade, Serbia
[d] University of Belgrade, "Vinča" Institute of Nuclear Sciences, P.O. Box 522, 11001 Belgrade, Serbia

ARTICLE INFO

Article history:
Received 4 May 2016
Received in revised form 2 June 2016
Accepted 28 June 2016
Available online 30 June 2016

Keywords:
Chitosan microparticles
Colloidal TiO_2
Azo dyes
Photocatalytic degradation
Reproducibility

ABSTRACT

The present paper deals with removal and photocatalytic degradation of the textile dyes by TiO_2 nanoparticles immobilized onto chitosan-based microparticles. The microparticles composed of chitosan (Ch) and poly(methacrylic acid) (PMA) were fabricated for the first time by inverse suspension polymerization. They were utilized for colloidal TiO_2 nanoparticles immobilization, synthetized by acidic hydrolysis of $TiCl_4$. To evaluate the potential application of Ch/PMA/TiO_2 microparticles for treatment of textile wastwaters, their photocatalytic activity was examined by degradation assessment of three different groups of anionic azo dyes in aqueous solutions under solar light simulating source. FTIR analysis revealed that Ch and PMA were incorporated in the polymer network. SEM and optical microscopy confirmed their spherical shape. Under illumination, Ch/PMA/TiO_2 microparticles completely removed dyes C.I. Acid Orange 7, C.I. Acid Red 18, C.I. Acid Blue 113, C.I. Reactive Black 5, C.I. Direct Blue 78, while removal degree of C.I. Reactive Yellow 17 was 75%. It was found that pH had significant influence on the photocatalytic activity of Ch/PMA/TiO_2 microparticles. Increase of solution pH from acidic to alkaline, lead to decrease in photodegradation rate of C.I. Acid Orange 7 during the first hours of illumination. After three illumination cycles, removal degree of C.I. Acid Orange 7 was maintained at remarkably high level (95% at pH 5.60 and 100% at pH 2.00 and 8.00), indicating that microparticles could be reused without significant loss of photocatalytic efficiency.

1. Introduction

Chitosan is natural, biodegradable polymer produced by deacetylation of chitin [1,2]. It is β-(1,4)-linked polysaccharide of D-glucosamine. Chitosan is a nontoxic, biodegradable and biocompatible natural polymer [3]. It is derived from naturally occurring sources, which are exoskeleton of insects, crustacean such as crabs, shrimps, prawns, lobsters and cell walls of some fungi [4].

* Corresponding author.
E-mail address: meli@tmf.bg.ac.rs (M. Kalagasidis Krušić).

http://dx.doi.org/10.1016/j.eurpolymj.2016.06.026
0014-3057/

Chitosan could be a material of choice for development of micro/nanoparticles since it has many advantages which include: (a) its ability to be used as a matrix for different organic and inorganic species and capability to control the release of active agents; (b) it is possible to avoid the use of hazardous organic solvents while fabricating particles, since it is soluble in aqueous acidic solution; (c) it is a linear polyamine containing a large number of free amino groups that are readily available for crosslinking; (d) its cationic nature allows ionic crosslinking with multivalent anions [1–3,5–7]. The methods employed for generation of chitosan micro- and nanoparticles include ionotropic gelation, complex coacervation, emulsion and microemulsion techniques, and self-assembling of hydrophobically modified chitosan [7–10].

In the present paper, chitosan microparticles with methacrylic acid were prepared by inverse suspension polymerization, where a water-soluble monomer and polymer are dispersed in a continuous organic phase. The advantage of inverse suspension over other polymerization methods is that a fine powdery product can be obtained and the particle size can be easily controlled by controlling the reaction conditions. Emulsifier concentration is usually between 1 and 5 wt% of the organic phase (below the critical micelle concentration). The dispersion is thermodynamically unstable and requires continuous vigorous agitation [11]. Further, methacrylic acid is widely used for the preparation of pH-sensitive hydrogels because it is biocompatible and can be copolymerized easily. If this acid is incorporated into hydrogels, even in very small amounts, the swelling behavior of hydrogels is significantly changed at appropriate pH values due to the ionization of COOH groups.

Applications of chitosan microparticles are ranging from pharmaceutical (e.g. drug delivery systems) to wastewater treatment, where they are used as sorbents for heavy metal ions or for sorption of various textile dyes [12]. Dyes pose a serious environmental hazard since colored wastewater can block both sunlight penetration and oxygen dissolution, essential for aquatic life [13,14]. Chitosan microparticles could also be used in photocatalytic degradation processes as matrices for immobilization of photocatalysts. The most common semiconductor used as a photocatalyst is titanium dioxide (TiO_2) as it is inexpensive, widely abundant, photochemically stable, non-toxic and water insoluble under most environmental conditions [15–17]. Major advantage of TiO_2 nanoparticles (NPs) immobilization onto supporting matrices, in case of the chitosan/poly(methacrylic acid) microparticles, is that liquid–solid separation is less expensive and much easier [18].

In our previous work, we successfully prepared hydrogel based on chitosan, itaconic and methacrylic acid in the form of a disk that was modified with synthetized colloidal TiO_2 NPs and commercial Degussa P25 [19,20]. This TiO_2/hydrogel nanocomposite has been used for investigation of photocatalytic degradation of three different groups of anionic azo dyes (acid, reactive and direct) in aqueous solutions under solar light simulating source. Under UV illumination, nanocomposite with immobilized colloidal TiO_2 NPs completely removed dyes C.I. Acid Orange 7, C.I. Acid Red 18, C.I. Acid Blue 113, C.I. Reactive Black 5, C.I. Direct Blue 78, while removal degree of C.I. Reactive Yellow 17 was 55%.

In the present study matrix for immobilization of TiO_2 NPs was synthetized in the form of microparticles in order to evaluate whether size and form of carrier had influence on photocatalytic activity of immobilized TiO_2 NPs. To our knowledge, applied method for fabrication of chitosan microparticles has not been reported in literature. Major advantage of microparticles usage in wastewater treatment and utilization for immobilization of TiO_2 NPs over classic hydrogel disk is their higher surface area (surface/volume ratio). In this form larger surface is available for immobilization of TiO_2 NPs which could enable faster photocatalytic degradation of water pollutants.

The microparticles composed of chitosan and poly(methacrylic acid) (Ch/PMA) were synthetized by inverse suspension polymerization. Colloidal TiO_2 nanoparticles, synthetized by acidic hydrolysis of $TiCl_4$, were immobilized onto Ch/PMA microparticles and their photocatalytic activity was investigated. Ch/PMA and Ch/PMA/TiO_2 microparticles were characterized using a Fourier transform infrared spectroscopy (FTIR), field emission scanning electron microscopy/energy dispersive X-ray (FE-SEM/EDX), optical microscopy and nitrogen adsorption-desorption isotherms. Photocatalytic degradation of six textile dyes (acid dyes C.I. Acid Orange 7, C.I. Acid Red 18, C.I. Acid Blue 113, reactive dyes C.I. Reactive Yellow 17, C.I. Reactive Black 5, direct dye C.I. Direct Blue 78) in aqueous solution was investigated in the presence of Ch/PMA and Ch/PMA/TiO_2 microparticles under solar light simulating source. In order to compare the effects, the experiments were also performed in the dark.

2. Experimental

2.1. Materials

Chitosan (Ch, Fluka, middle viscous) and methacrylic acid (MA, Sigma A.G.) were used for the synthesis of microparticles. In order to remove inhibitor, MA was vacuum distillated before use. The crosslinking agent *N*,*N*′-methylenebisacrylamide (MBA, Acros), initiator potassium persulfate (KPS, Merck, p.a.) and catalyst tetramethylethylenediamine (TEMED, Acros Organics, p.a.) were applied without purification. Paraffin oil (Centrohem) was used as an organic solvent for the formation of the water in oil inverse suspension polymerization system, and the surfactant was Tween80 (Reidel de Haen). Deionized water was used in all experiments. Buffer solutions were prepared using hydrochloric acid (HCl, Centrohem, p.a.) and potassium chloride (KCl, Carlo Erba, p.a.). pH of dye solution was adjusted with HNO_3 and NaOH solutions.

Six textile dyes were tested during photodegradation experiments: three acid dyes C.I. Acid Orange 7, C.I. Acid Red 18 and C.I. Acid Blue 113, two reactive dyes C.I. Reactive Yellow 17 and C.I. Reactive Black 5 and one direct dye C.I. Direct Blue 78. Maximum absorption wavelength (λ_{max}) of each dye is given in Table 1, while their structures are shown in Fig. 1.

Table 1
List of anionic azo dyes used in the study.

Anionic textile dye	Abbr.	Supplier	λ_{max} (nm)	M.W. (g mol^{-1})	pH of dye solution
C.I. Acid Orange 7	AO7	Cassela	486	350.3	5.60
C.I. Acid Red 18	AR18	Cassela	507	604.4	6.10
C.I. Acid Blue 113	AB113	Cassela	567	681.8	6.30
C.I. Reactive Yellow 17	RY17	Höchst AG	430	682.7	7.50
C.I. Reactive Black 5	RB5	Höchst AG	590	991.8	6.20
C.I. Direct Blue 78	DB78	Bezema AG	603	1055.9	5.60

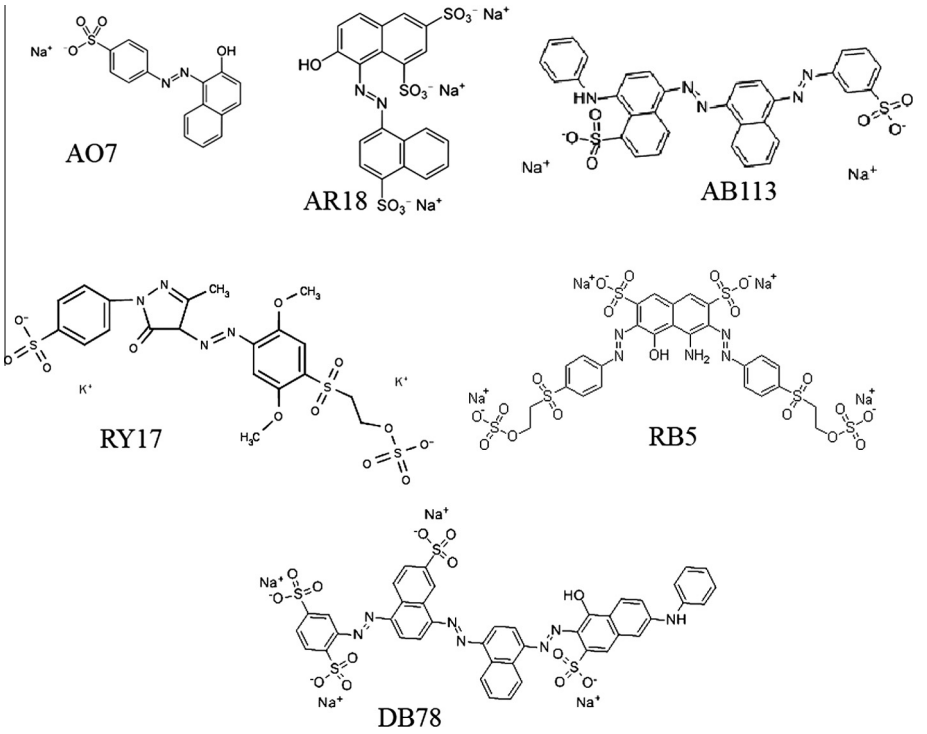

Fig. 1. Structures of studied dyes.

2.2. Synthesis of colloidal TiO_2 NPs

As a photocatalyst, colloidal TiO_2 NPs were employed throughout the photodegradation experiments. Detailed synthesis of colloidal TiO_2 NPs by acidic hydrolysis of $TiCl_4$ is previously described [21]. The colloid was prepared in a manner analogous to the one proposed by Rajh et al. [22]. The solution of $TiCl_4$ cooled down to −20 °C was added drop-wise to cooled water (at 4 °C) under vigorous stirring and then kept at this temperature for 30 min. The pH of the solution was between 0 and 1, depending on $TiCl_4$ concentration. Slow growth of the particles was achieved by dialysis against water at 4 °C until the pH of the solution reached 3.5. The concentration of colloid was determined from the concentration of the peroxide complex obtained after dissolving the particles in concentrated sulfuric acid [23]. In order to enhance the crystallinity and overall efficiency of generated TiO_2 NPs the colloid was thermally treated in reflux at 60 °C for 16 h. The synthesized colloid comprises of faceted, single crystalline, anatase TiO_2 NPs with an average size of 6 nm [21].

2.3. Synthesis of Ch/PMA and Ch/PMA/TiO_2 microparticles

The microparticles were synthesized by an inverse suspension polymerization in paraffin oil using Tween80 as an inverse suspension stabilizing agent. The polymerization was carried out in a three-necked flask equipped with a mechanical stirrer, a thermostatically controlled water bath, and a nitrogen duct. Water and oil phases were mixed in 1:10 ratio. The stabilizer Tween80 was dissolved in paraffin oil for the preparation of the continuous phase. 0.2 g of Ch was dissolved in 2 mL of MA and 6 mL of deionized water. The crosslinking agent, MBA, was added to the Ch solution, until the concentration reached 5 wt% with respect to the total weight of the monomer. When the reaction mixture became homogenous, 0.04 g of initiator KPS was added to the reaction mixture, which was purged with N_2.

This mixture was added drop-by-drop to the continuous medium in the flask. Afterwards, complete mixture was stirred (450 rpm) for 15 min at 50 °C and purged with nitrogen and then 0.1 mL of TEMED was dropped into the reactor. The polymerization was continued in the next 3 h. In order to remove non-reacted chemicals, oil, and surfactant, the obtained microparticles were washed out three times using petroleum ether and deionized water, respectively. The microparticles were dried in the oven at 37 °C for 24 h and kept in a desiccator at 25 °C until further use.

Immobilization of the photocatalyst NPs was performed by the dip-coating method. This method relies on the immobilization of TiO_2 NPs onto microparticles by immersing the blank sample into photocatalyst colloid solution. 0.1 M colloid solution of synthetized TiO_2 NPs was used for microparticle modification. Ch/PMA microparticles were left to swell for 2 h in photocatalyst colloid solution and subsequently dried at room temperature until the constant weight was obtained. Afterwards, samples were left 30 min at 80 °C and then rinsed twice (5 min) with deionized water and dried at room temperature.

In further text, the Ch/PMA sample (without photocatalyst nanoparticles) will be marked as *B*, while the Ch/PMA/TiO_2 sample (with immobilized photocatalyst nanoparticles) will be marked as *B*-0.1TiO_2.

2.4. Characterization

Fourier transform infrared (FT-IR) spectra were recorded by Bomem MB 100 FT-IR spectrophotometer in the region 4000–400 cm^{-1}. The samples were prepared in the form of pellets with KBr at room temperature and measured in transmission mode.

Data related to macroscopic structure of microparticles were obtained using optical microscope AxioImager A1 with an AxioCam HRc camera and AxioVision digital image processing software (Carl Zeiss, Germany). Ch/PMA microparticles were examined immediately after synthesis (native microparticles), in dry and in swollen form (dry particles immersed in buffer of pH 2.00, until the equilibrium degree of swelling was achieved). Also, Ch/PMA/TiO_2 microparticles were investigated in swollen and in dry state. Average microparticle diameter was calculated using software *ImageJ*.

Microparticle morphology was characterized by scanning electron microscopy (FE-SEM, Tescan Mira 3XMU). Presence of TiO_2 was determined in energy-dispersive X-ray (EDX) spectroscopy mode using JEOL JSM-5800 scanning electron microscope. Prior to SEM analysis samples were coated with gold/platinum alloy (15/85) under vacuum conditions, using Polaron SC502 vacuum sputter coater.

Nitrogen adsorption-desorption isotherms were determined using a Micromeritics ASAP 2020 instrument. Samples were degassed at 105 °C for 10 h under reduced pressure. The specific surface area of samples was calculated according to the Brunauer, Emmett, Teller (BET) method from the linear part of the nitrogen adsorption isotherms. The total pore volume was given at $p/p_0 = 0.998$. The volume of the mesopores was calculated according to the Barrett, Joyner and Halenda method from desorption branch of the isotherm [24]. The volume of micropores was calculated from the alpha-S plot.

2.5. Experiment in the dark and photodegradation experiments

To evaluate the adsorption capacity and photocatalytic activity of the prepared samples, several azo dyes were employed as model organic pollutants. In order to test whether selected dyes are prone to photodegradation under UV irradiation, photolysis test was carried out without any catalyst. 25 mL of each dye solution was placed under lamp without addition of photocatalyst and change of concentration was monitored using UV/VIS spectrophotometer.

To investigate the photocatalytic efficiency of prepared samples for photodegradation of selected dyes, batch experiments were set up, where defined amount of sample *B* and *B*-0.1TiO_2 was placed in beaker with dye solution. Batch experiments (at native pH of each dye solution) were carried out in two different conditions:

(i) In the dark (by closing the lid of the mechanical shaker in which the experiment was conducted) in order to evaluate sorption ability of prepared samples for selected azo dye.
(ii) Under illumination provided by ULTRA-VITALUX lamp, 300 W (Osram); the lamp simulated sun-like irradiation with a spectral radiation power distribution at wavelengths between 300 and 1700 nm. The distance between the lamp and sample was set to 30 cm. Optical power was measured using R-752 Universal Radiometer Readout with sensor model PH-30, DIGIRAD and it was 30 mW cm^{-2}.

During both experiments, 0.2 g of sample was placed in a beaker with 25 mL of dye solution (initial concentration was 10 mg L^{-1}) and then beaker was transferred in water bath with mechanical agitation at 25 °C. In the first 8 h (1–4, 6 and 8 h), 3 mL of solution was taken to monitor the remaining dye concentration by an UV/VIS spectrophotometer Cary 100 Scan (Varian), at a maximum absorption wavelength of each dye. The aliquot was then returned to the sample. Afterwards, samples were left in the beakers for the next 16 h. The average percentage of dye removal from solution was calculated by equation:

$$D\ (\%) = \frac{C_0 - C_t}{C_0} \cdot 100 \tag{1}$$

where C_0 and C_t (mg L^{-1}) are the initial dye concentration and dye concentration at time *t*, respectively.

Based on the photodegradation experiments, the dye that showed the best results was chosen for further investigation of pH influence on the photodegradation efficiency of the *B*-0.1TiO_2 sample. pH of dye solution was adjusted to 2.00 and 8.00 by 0.1 M HNO_3 and 0.1 M NaOH solution, respectively. The reproducibility of photocatalytic activity of the sample *B*-0.1TiO_2 was tested in two more cycles under the same conditions (in the fresh 25 mL of dye solution that showed the best results in the first photodegradation cycle).

3. Results and discussion

3.1. Structural and morphological characterization of Ch/PMA and Ch/PMA/TiO_2 microparticles

To our knowledge, an inverse suspension polymerization was used for the first time to obtain microparticles of chitosan with methacrylic acid. Resulting products were particles of spherical shape in the form of a fine powdery, non-transparent and white, confirming that chitosan-based microparticles were successfully prepared by this method. The prepared particles were further used as a matrix for immobilization of the TiO_2 nanoparticles.

An optical microscope was used to obtain information about macroscopic structure of microparticles, such as shape, size, average diameter and agglomeration. Blank microparticles (*B*) were examined immediately after synthesis – "as synthesized" microparticles, in a dry and swollen form (Fig. 2a–c). Hydrogel microparticles with average diameter of approximately 400 μm were spherical (Fig. 2a) immediately after synthesis. After drying the microparticles shrunk to irregular shape (Fig. 2b), but they did not agglomerate. When *B* microparticles were reimmersed in a buffer solution (pH 2.00), their shape recovered and they became spherical again (Fig. 2c). The diameter of rehydrated microparticles (≈550 μm) was larger compared to diameter of microparticles after synthesis due to swelling in buffer solution.

B-0.1TiO_2 microparticles were investigated in swollen state immediately after immobilization of TiO_2 NPs and in a dry state. As shown in Fig. 2d, these microparticles were also spherical with diameter similar to those of the swollen *B* microparticles. On the other hand, when these samples were dried (Fig. 2e), their structure remained spherical, maybe due to the swelling and deswelling process.

Morphology of microparticles was assessed by FE-SEM analysis. Fig. 3 shows the micrographs of the *B* and *B*-0.1TiO_2 microparticles, and their magnified surfaces. Evidently, microparticles are spherical with dense morphology (Fig. 3).

EDX spectra of the *B* and *B*-0.1TiO_2 samples are shown in Fig. 4a and b. The peaks corresponding to Ti in EDX spectrum of the *B*-0.1TiO_2 sample confirmed the presence of TiO_2 NPs on the surface microparticles.

The shape of N_2 isotherms (not shown) implied high mesoporosity of the *B*-0.1TiO_2 microparticles with relatively high specific surface area of 5.04 and 1.67 $m^2\,g^{-1}$ and the total pore volume $5.11{\cdot}10^{-3}$ and $8.18{\cdot}10^{-4}\,cm^3\,g^{-1}$ for *B* and *B*-0.1TiO_2 samples, respectively. Mean pore diameter of *B*-0.1TiO_2 sample was around 3.18 nm and the largest number of pores had diameter of 2.90 nm indicating that pore size was mainly uniform in the microparticles. On the other hand, it was not possible to determine the pore size of the blank microparticles.

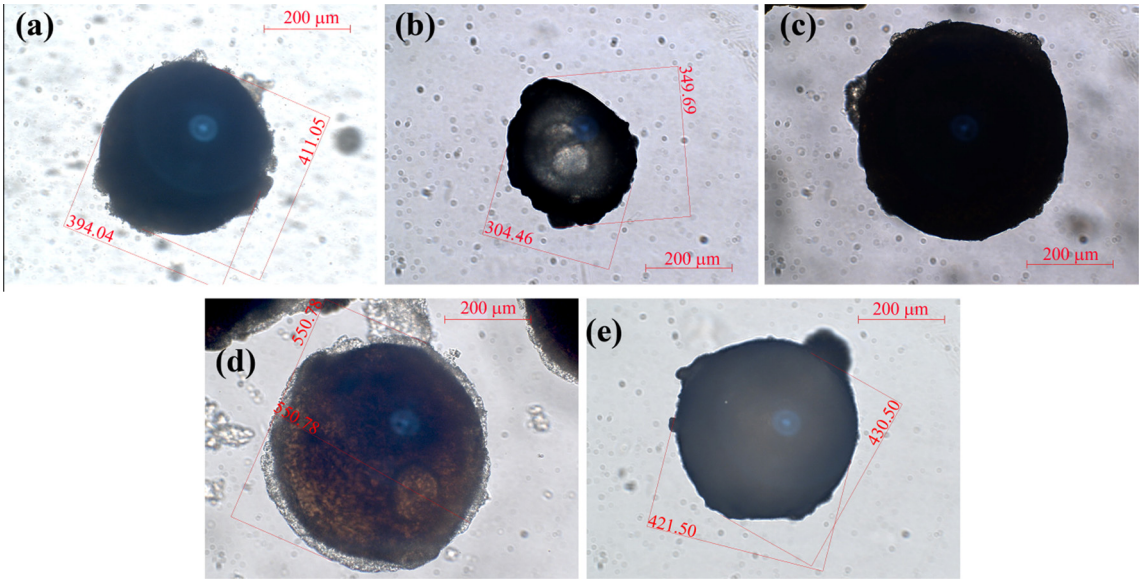

Fig. 2. Microphotographs of *B* microparticles: (a) "as synthesized" microparticle; (b) dry microparticle; (c) swollen microparticle and B-0.1TiO_2; (d) after immobilization; (e) dry microparticle.

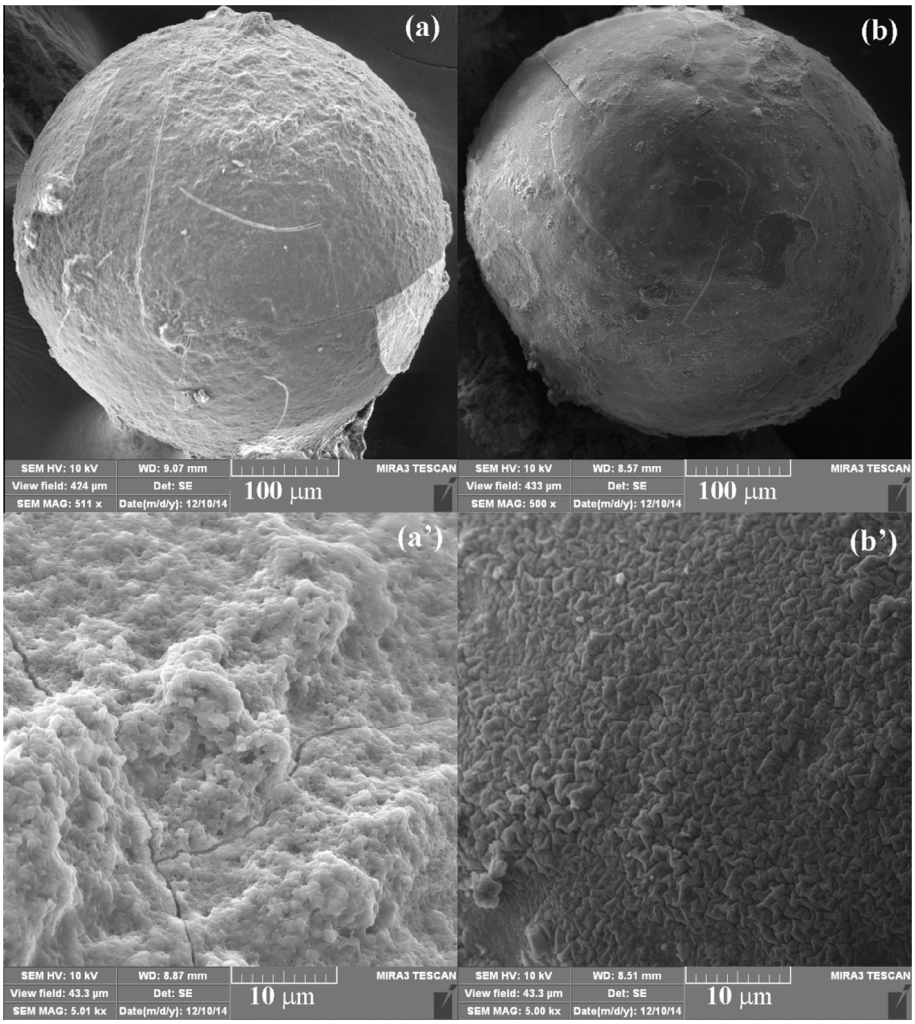

Fig. 3. SEM micrographs of samples: (a, a') *B* and (b, b') *B*-0.1TiO_2.

The FTIR analysis of the *B* and *B*-0.1TiO_2 microparticles is shown in Fig. 5. The bands at 3424 cm^{-1} in the spectrum of the *B* sample and at 3431 cm^{-1} in spectrum of the *B*-0.1TiO_2 sample could be assigned to the axial stretching vibrations of OH groups superimposed to the N—H stretching bands and intermolecular hydrogen bonds of polysaccharide [25]. The CH stretching vibration of methyl groups and bending vibration of —CH_2 groups in chitosan were observed around 2900 cm^{-1} in spectra of both samples, *B* and *B*-0.1 TiO_2 [26,27]. The band at 1653 cm^{-1} in spectrum of the *B* sample is assigned to C═O stretching band (amide I) while the band at 1698 cm^{-1} is ascribed to the carboxylic groups in methacrylic acid [28]. The band which appeared at 1259 cm^{-1} in spectrum of the *B* sample has been reported as the amide II C—N bonds in chitosan [29]. The band emerging at 1072 cm^{-1} in spectrum of the *B* sample, characteristic for polysaccharide and attributed to the C—O stretching vibration from β (1 → 4) glycosidic bonds, was shifted to 1090 cm^{-1} in spectrum of the *B*-0.1 TiO_2 sample [28].

Comparing the FTIR spectra of the hydrogel before and after immobilization of TiO_2 NPs, few changes in spectrum of the *B*-0.1 TiO_2 sample were observed. These changes could be an indication of interaction between microparticles and OH groups on the surface of TiO_2 NPs. Intense peak at 1707 cm^{-1} in spectrum of the *B*-0.1 TiO_2 sample, assigned to C═O stretching vibration, implies the formation of esters i.e. ester bond (—CO—O—) between carboxylic groups of methacrylic acid and surface OH groups of TiO_2 NPs [28,30]. The formation of ester bond is followed by increase in the intensity of the peak at 1180 cm^{-1} which is assigned to the ester C—O stretching vibration [27] and decrease in intensity of peak 1541 cm^{-1} assigned to the asymmetric stretching vibration of COO^- group of methacrylic acid [30]. Finally, band of medium intensity which appeared in spectrum of the *B*-TiO_2 sample at 1389 cm^{-1} is characteristic of symmetric stretching vibration of C═O group in formed unidentate carboxylate (—CO—O—Ti—) [30].

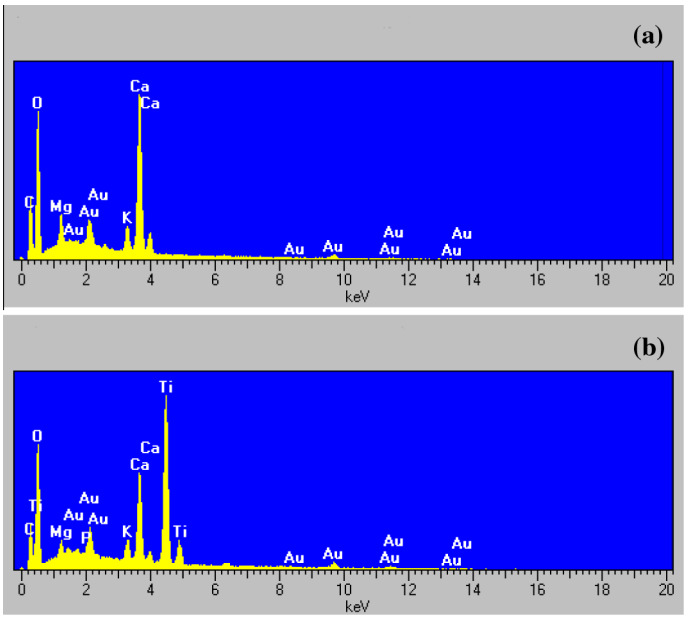

Fig. 4. EDX spectra of samples: (a) *B* and (b) *B*-0.1TiO_2.

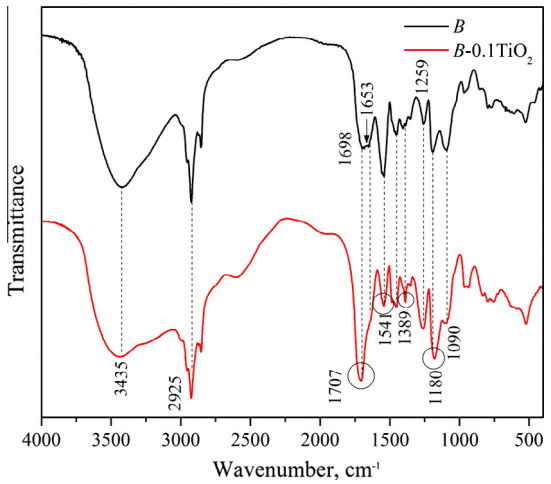

Fig. 5. FTIR spectra of the samples *B* and *B*-0.1TiO_2.

3.2. Removal of anionic azo dyes from aqueous solution by synthetized microparticles

Dye adsorption ability of microparticles and photocatalitic activity of immobilized TiO_2 NPs were tested with six textile dyes: acid dyes AO7, AR18 and AB113, reactive dyes RY17 and RB5, and direct dye DB78. In order to establish the possible contribution of dye degradation only due to exposure to light, dye solutions were illuminated for 24 h under the same conditions as the photodegradation experiments. Change of AO7, AR18, RY17 and DB78 concentrations in the solution were not observed in investigated time interval. However, it was found that after 24 h long illumination photolysis degradation rates for RB5 and AB113 were around 10 and 21%, respectively [20].

3.2.1. Removal of acid azo dyes

The results of acid dyes AO7, AR18 and AB113 removal from aqueous solution in the dark and under illumination by the *B* and *B*-0.1TiO_2 samples are shown in Fig. 6 along with photographs of samples after 24 h for both experiments. Removal of the dyes in the dark was performed to evaluate sorption efficiency of the prepared sample. In this case, in the absence of the UV light necessary to initiate photodegradation process by TiO_2 NPs, only sorption of the dye by samples occurred. On the other hand, when samples were illuminated with ULTRA-VITALUX lamp, due to presence of TiO_2 NPs photodegradation of

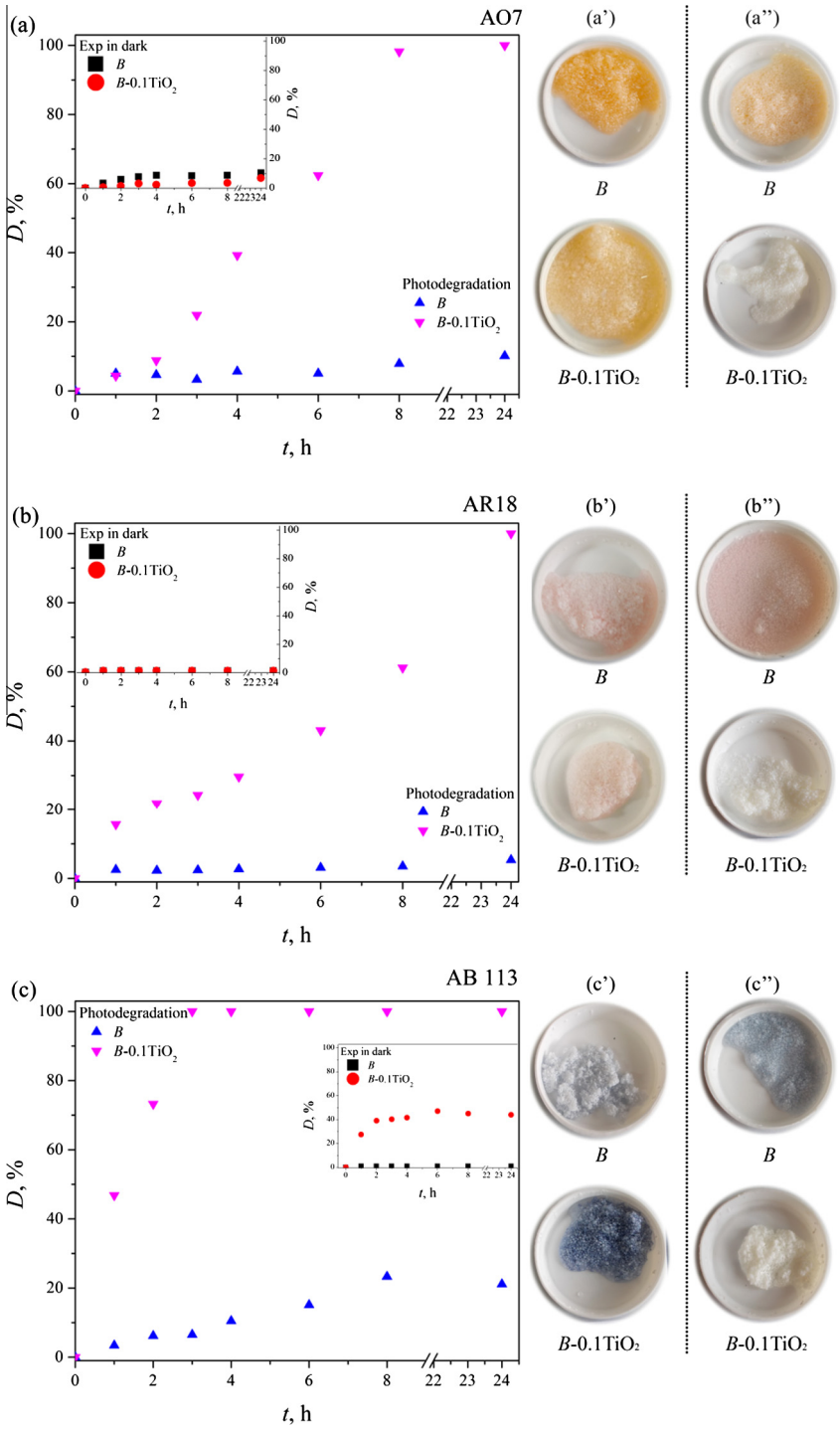

Fig. 6. (a) Removal of dye AO7 and corresponding images of samples after 24 h of experiment in the dark (a') and under illumination (a''); (b) removal of dye AR18 and corresponding images of samples after 24 h of experiment in the dark (b') and under illumination (b''); (c) removal of dye AB113 and corresponding images of samples after 24 h of experiment in the dark (c') and under illumination (c'').

dyes takes place along with the sorption. In order to confirm the given explanation, together with diagrams that show decrease of dye concentration in solution, images of samples are given to show that there was no color on the microparticles for the most of the investigated dyes [31,32].

Blank sample showed low sorption affinity for the dye AO7 in the dark (Fig. 6a, insert), while there was negligible sorption of the dyes AR18 and AB113 (Fig. 6b and c, insert). It is well known that the structure and ionic charge of the dye play an intrinsic role in the sorption of acid dyes on chitosan [33]. Several studies reported that 1:1 stoichiometry between protonated amino groups in chitosan and sulfonate groups of acid dyes could be expected [33,34]. Dye AO7 possess only one sulfonate group and thus, it was better sorbed than AR18 or AB113 which have two or three sulfonate groups in their structure, respectively. In other words, the affinity decreases with an increase in degree of sulfonation of the dye and after the first sulfonate group, each additional group has a negative influence on the sorption, facilitating the desorption of the dye [35].

The *B* sample did not contain TiO_2 NPs and thus, photodegradation of the dyes could not occur (Fig. 6a''–c''). This is illustrated by photographs taken after 24 h of illumination experiment, especially for dye AO7, where it can be seen that the *B* sample sorbed dye to some extent under illumination, but it remained colored after 24 h (no photodegradation occurred). The amount of adsorbed dye AO7 under illumination is equivalent to the amount adsorbed in the dark. However, removal of dye AB113 was changed compared to the experiments in the dark. Unlike the experiments in the dark, the *B* sample removed ≈20% of dye AB113 after 24 h of degradation, but this is attributed to the photolysis since photographs of the *B* after 24 h did not show color on microparticles (Fig. 6c'').

The *B*-0.1TiO_2 sample exhibited similar behavior as the *B* sample during the experiment in the dark, where low sorption of AO7 (approximately 4%) and negligible sorption of AR18 were detected in the dark (Fig. 6a and b, insert). Possible explanation for this kind of behavior could be associated to the pH of AO7 and AR18 solutions.

pH value of AO7 dye solution was 5.60 (Table 1), while the pK_a of chitosan has been reported to be in the range of 6–6.5 [36]. At this pH all amino groups of chitosan are present in protonated ($—NH_3^+$) causing a certain sorption affinity.

pH value of AR18 solution was 6.1 (Table 1), and at this pH both forms of amino groups in chitosan (protonated ($—NH_3^+$) and neutral form ($—NH_2$)) are present. In such conditions protonated form of amino groups as sorption cites for dye anions are not dominant which explained low sorption of AR18. In addition, pH 6.2 represents the point of zero charge of TiO_2 NPs nanoparticles [37,38]. Hence, at this pH value hydroxyl groups are not available for binding of dye anions.

On the other hand, sorption of AB113 in the dark by sample *B*-0.1TiO_2 at pH 6.3 significantly increased. For explanation of this observation it should be also taken into account the molecular structure of AB113 dye (Fig. 5). Namely, it could be expected more uniform spreading of negative charge in dye molecule which contributes to efficient interaction with surface species present in chitosan and TiO_2 nanoparticles.

When the *B*-0.1TiO_2 sample was illuminated with ULTRA-VITALUX lamp, complete removal of the dye AO7 was achieved already within first 8 h of illumination. Confirmation for this result is given in Fig. 6a, where it can be seen that complete discoloration of the dye AO7 solution was obtained and absence of color on microparticles (Fig. 6a'') indicated that photodegradation of dye was efficient and successful. On the other hand, the *B*-0.1TiO_2 sample removed approximately 60% of dye AR18 within the first 8 h of illumination. It is evident that the next 16 h of illumination were needed to complete the removal of this dye, which was also confirmed by image of the samples (Fig. 6b''). Slower degradation of AR18 compared to AO7 could be explained by the difference in molecular structure of these dyes (Fig. 5). As already mentioned, the structure of the dye significantly affects the process of adsorption. Therefore, such behavior could be attributed to slower adsorption of AR18 and its possible desorption due to three sulfonate groups in its structure. The *B*-0.1TiO_2 sample rapidly removed 100% of AB113 from the solution (complete removal occurred after 3 h, Fig. 6c). This is likely due to the synergetic effect of photolysis, sorption and photodegradation under illumination.

3.2.2. Removal of reactive azo dyes

The results on removal of reactive dyes RY17 and RB5 from solutions are demonstrated in Fig. 7. Low sorption of RY17 and RB5 took place in the dark with both, *B* and *B*-0.1TiO_2 samples. Photographs of the samples are in good correlation with the results presented in Fig. 7a and b. This is likely due to the fact that pH of the RY17 solution was even higher compared to acid dyes, at which majority of amino groups was in $—NH_2$ form. Consequently, they could not establish interaction with dye that is in anionic form. On the other hand, $—O^-$ was present on the surface of TiO_2 NPs and carboxylic groups of methacrylic acid in COO^- form, causing the repulsion between negatively charged nanoparticles surface and dye anions. pH value of RB5 solution was similar to the pH of AR18 and hence sorption of dye was not favored process.

As expected, even when it was exposed to illumination the *B* sample did not remove dye RY17 from solution. In contrast, the *B*-0.1TiO_2 microparticles removed approximately 40% of dye within the first 8 h of illumination. Higher removal degree was obtained in the following 16 h (75% in total, Fig. 7a). As can be seen from Fig. 7a'', the sample remained only slightly colored meaning that not only the dye from solution did not degrade but also the part of the dye which was adsorbed on the microparticle. Slight removal of dye RB5 under illumination in the presence of the *B* sample was due to photolysis. The photograph of the *B* sample after 24 long illumination was almost the same as the one made after 24 h long adsorption in the dark (Fig. 7b''). Removal degree of dye RB5 by the *B*-0.1TiO_2 sample after 8 h long illumination was 60%. Complete photodegradation occurred in the next 16 h (Fig. 7b). Efficient degradation of the dye RB5 was also confirmed by complete discoloration of the *B*-0.1TiO_2 sample (Fig. 7b''). Larger removal of the dye RB5 in comparison with the dye RY17 could be explained by differences in dye structures. Dye RB5 has two azo, two vinylsulfonate and hydroxyl groups, which are susceptible to photolytic and photocatalytic degradation [39].

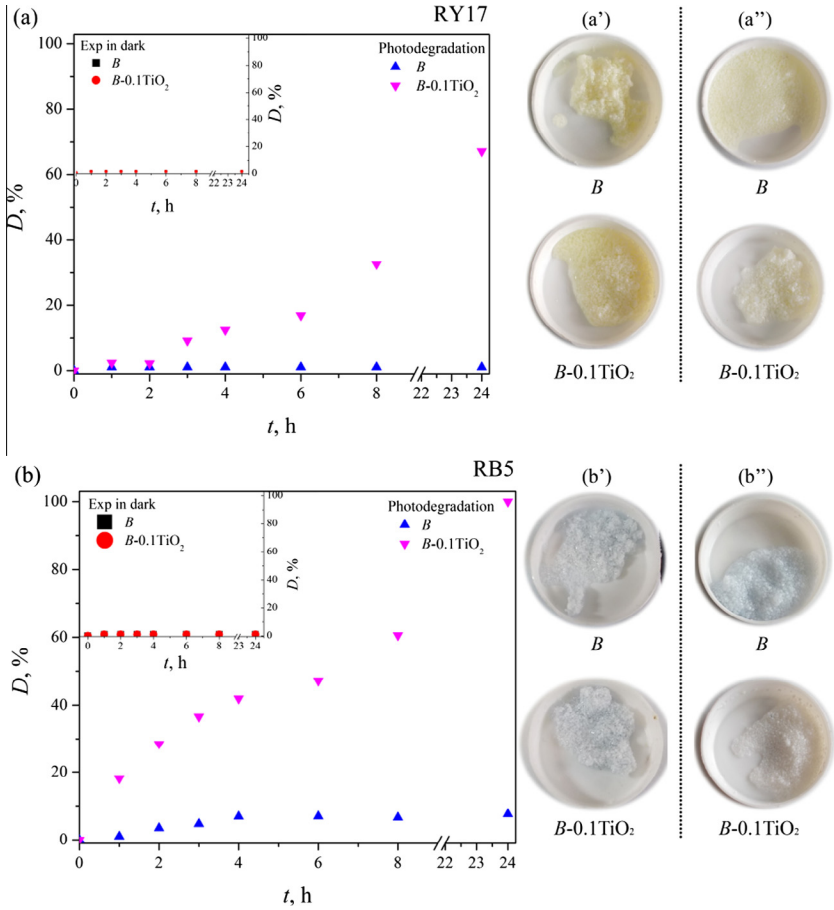

Fig. 7. (a) Removal of dye R17 and corresponding images of samples after 24 h of experiment in the dark (a') and under illumination (a''); (b) removal of dye RB5 and corresponding images of samples after 24 h of experiment in the dark (b') and under illumination (b'').

3.2.3. Removal of direct azo dyes

Experiments in the dark pointed out that prepared samples exhibited poor sorption affinity for the dye DB78 on both *B* and *B*-0.1TiO_2 samples (Fig. 8a, insert). This result was expected taking into account the size of dye molecule and the fact that it contains four sulfonic groups which are enhancing its solubility in water (Fig. 5). Likewise, *B* sample did not remove dye

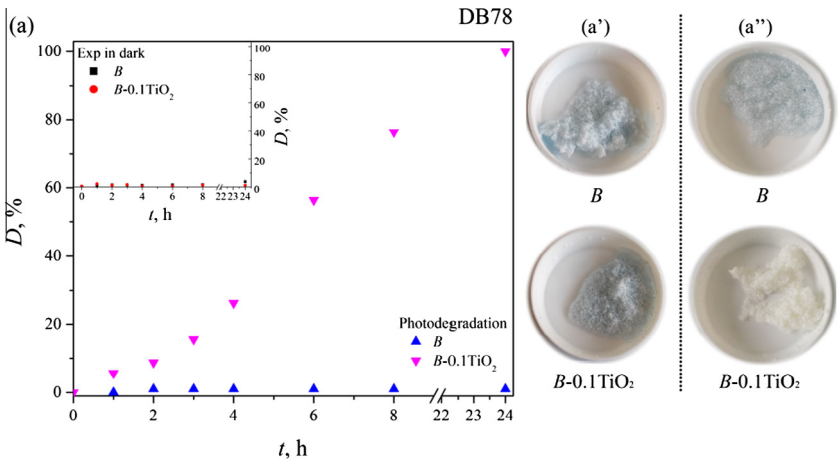

Fig. 8. (a) Removal of dye DB78 and corresponding images of samples after 24 h of experiment in the dark (a') and under illumination (a'').

during illumination. However, under the same conditions the *B*-0.1TiO_2 sample removed approximately 80% of dye within the first 8 h of experiment, while the complete photodegradation of the dye DB78 was obtained after 24 h. The *B*-0.1TiO_2 sample was completely discolored after 24 h of illumination (Fig. 8a'').

3.2.4. Influence of pH on the removal of AO7

The pH of wastewater from textile industry significantly varies (from acidic to alkaline) depending on the used dyes and processes during dyeing of textiles. Photodegradation of dyes is affected by pH of the solution since it directly affects the surface charge of TiO_2 NPs and synthetized microparticles. Taking into account that dye AO7 was the most efficiently photodegraded one among all investigated dyes, we have chosen this dye for further investigation of influence of pH on photodegradation process. The results of removal behavior of AO7 by prepared samples in the dark and under illumination at pH 2.00 and pH 8.00 are shown in Fig. 9.

When pH of dye solution was adjusted to 2.00, removal behavior of microparticles was significantly changed compared to native pH 5.6 of dye solution in both cases, in the dark and under illumination (Fig. 6a). In this case, considerable amount of dye was sorbed in the dark. The *B* sample sorbed approximately 40% of dye within 24 h of experiment, while the sample *B*-0.1TiO_2 removed more than 90% (Fig. 9a, inset). Explanation for this behavior can be found in the fact that protonated form of amino groups (—NH_3^+) in chitosan prevailed at pH 2.00, enabling efficient interactions with negatively charged dye anions. On the other hand, enhanced sorption of dye on the *B*-0.1TiO_2 sample was a consequence of the presence of positively charged OH_2^+ groups on the surface of TiO_2 NPs. Photographs of both microparticles (Fig. 9a') also confirm these results, where it can be noticed that the *B*-0.1TiO_2 sample was more intensively colored compared to *B* sample.

When pH of dye solution was set to pH 8.00, similar removal behavior to the one at native pH solution was observed (Fig. 9b). As predicted, after 24 h long sorption in the dark slight sorption of dye AO7 by both samples occurred. At this

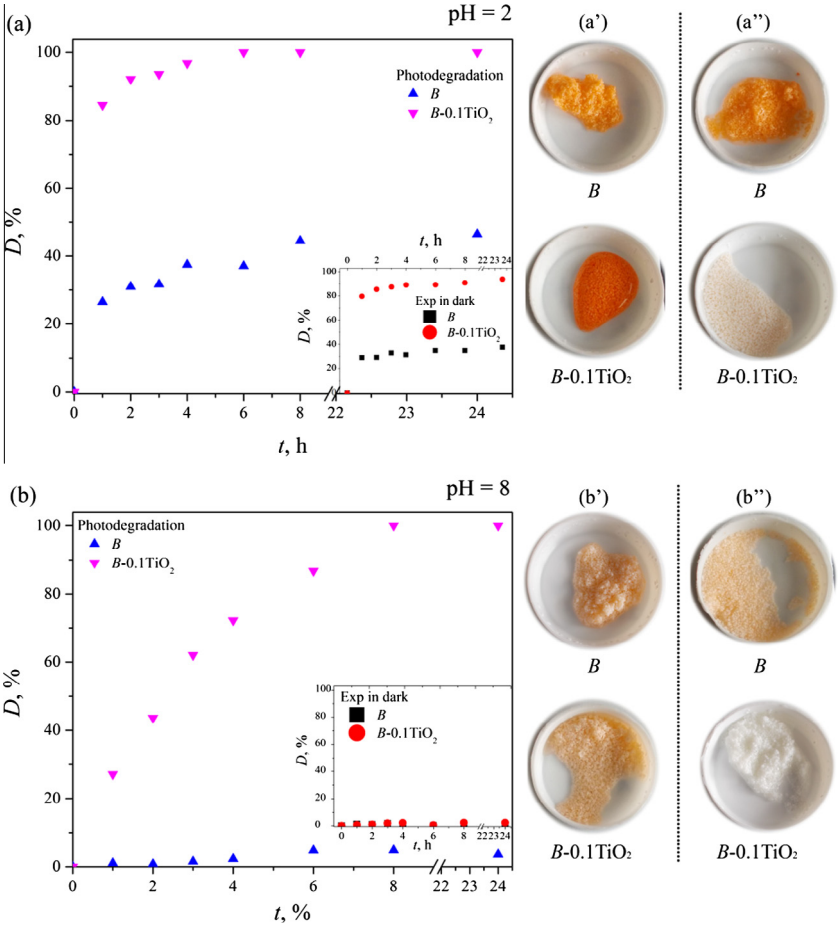

Fig. 9. (a) Removal of dye AO7 from the solution, when pH was adjusted to 2.00, and corresponding images of samples after 24 h of experiment in the dark (a') and photodegradation experiment (a''); (b) removal of dye AO7 from the solution, when pH was adjusted to 8.00, and corresponding images of samples after 24 h of experiment in the dark (b') and photodegradation experiment (b'').

Table 2
The effect of AO7 solution pH on sorption/photodegradation process by *B*-0.1TiO_2.

pH	Time of photodegradation experiment	
	8 h	24 h
2.00	Complete removal of dye from solution (within 2 h); almost complete sorption	*B*-0.1TiO_2 slightly colored indicating that photodegradation was not complete
5.60	Complete sorption and photodegradation	Complete sorption and photodegradation
8.00	Complete sorption and photodegradation; faster compared to pH 5.60	Complete sorption and photodegradation, faster compared to pH 5.60

pH, all amino groups are in the —NH_2 form and negative charge is present on the surface of TiO_2 NPs and methacrylic acid causing repulsion between dye anions and samples (Fig. 9b').

It should be noticed from Fig. 9a that both samples *B* and *B*-0.1TiO_2 at pH 2.00 exhibited almost the same behavior in process of dye removal under illumination and in the dark. The *B* sample removed 40% of dye due to sorption, but it did not degrade the dye. This result was confirmed by given images of sample after 24 h of illumination. Complete removal of dye AO7 from the solution by the *B*-0.1TiO_2 sample was achieved only after 6 h of illumination. However, photographs of sample showed that some dye remained in microparticles after 8 h of exposure to UV light (data not given), which indicates that photodegradation was not complete in this time interval. In the next 16 h of experiment, AO7 degradation in the sample was continued, but still even after 24 h some dye remained in the sample (Fig. 9a''). Dye molecules were probably trapped inside the microparticles and not exposed to TiO_2 NPs that slowed down degradation process.

An increase of pH of dye solution led to an increase of photodegradation rate compared to native pH, in the presence of the *B*-0.1TiO_2 sample. Faster initial removal was observed when pH of the solution was 8.00 compared to pH 5.60. Complete removal of dye from the solution and degradation of dye from the microparticles occurred after 8 h of illumination. This result could be explained the fact that dye cannot be trapped by microparticles, like in the case of pH 2.00, due to inappropriate charge which favored repulsion. More efficient removal of dye at pH 2.00 already after 1 h of illumination compared to the same process at pH 8.00 is clearly seen, Fig. 9. Similar behavior was observed in literature [40–42]. This could be expected taking into account the surface charge of the *B*-0.1TiO_2 sample and molecular structure and charge of dye at corresponding pH values. Namely, faster degradation will take place at lower pH of dye solution since the positively charged TiO_2 surface favors the adsorption of negatively charged dye anions and vice versa. However, in the system where chitosan is present, sorption of dye is also a factor that plays significant role, since dye is also located inside the microparticles and thus, photodegradation is hindered. Summary effect of AO7 solution pH on sorption/photodegradation process by *B*-0.1TiO_2 is given in Table 2.

3.2.5. Reproducibility study

Major benefit of TiO_2 NPs immobilization onto supporting material is simple and inexpensive recovery of photocatalyst. After the first illumination cycle was finished, the samples were collected and left to dry. Afterwards, the same samples were used in fresh batch of dye solution and illuminated again two times. Fig. 10 shows dye removal efficiency using the *B*-0.1TiO_2 sample during three photodegradation cycles. It is evident that photocatalytic removal degree was at remarkably high level

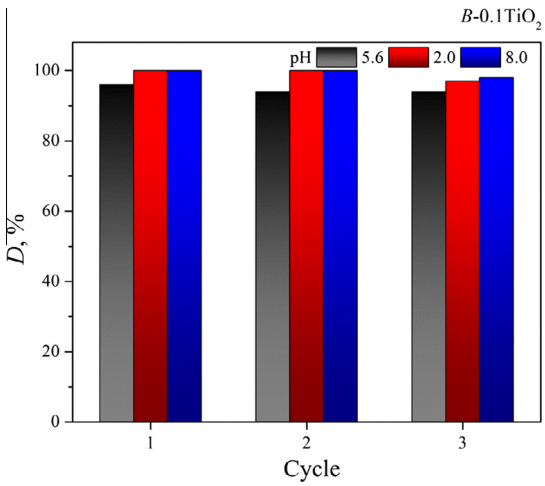

Fig. 10. Photodegradation efficiency of *B*-0.1TiO_2 samples after three cycles of UV illumination at pH 5.60, 2.00 and 8.00 (8 h of UV illumination, initial dye concentration: 10 mg L^{-1}).

for all three investigated pH values. When pH of dye solution was set to 8.00, complete removal of dye from solution and degradation occurred in all three samples (photographs of the samples are not shown). During two additional photodegradation cycles at pH 2.00, complete removal was observed, but as in the case of the first cycle, some dye was left in microparticles after cycle was finished. Only for pH 5.6 slight decrease in removal efficiency was observed, but complete photodegradation of dye sorbed on the microparticles occurred in all three cycles.

As already mentioned, in our previous research hydrogels based on chitosan, itaconic acid and methacrylic acid were synthetized in the form of disks and employed for immobilization of TiO_2 NPs (TiO_2/hydrogel nanocomposite) [19], while in the present study carrier was in the form of microparticle. Diameter and size of microparticles were much smaller in comparison with disks. Hence, higher specific surface was available for immobilization of TiO_2 NPs. A comparison of the results of photodegradation of AO7 dye by TiO_2 NPs modified disks [19] and microparticles indicates that much faster photodegradation process and higher photocatalytic activity after three repeating cycles of illumination, were achieved by TiO_2 modified microparticles.

Finally, taking into account all obtained results, several factors affect photocatalytic degradation of textile dyes by TiO_2 NPs immobilized onto hydrogel disk or microparticles: (a) a size and form of TiO_2 NPs carrier; (b) time needed for sorption/photodegradation process; (c) class of dye and (d) pH of dye solution. Therefore, faster photodegradation can be achieved by reduction of size and change of form (from hydrogels disk to microparticles) of TiO_2 NPs carrier. In addition, pH of dye solution affects both, the carrier and TiO_2 NPs, and hence sorption/photodegradation processes itself.

4. Conclusion

The microparticles composed of chitosan (Ch) and poly(methacrylic acid) (PMA) were synthetized by inverse suspension polymerization. Colloidal TiO_2 nanoparticles, synthetized by acidic hydrolysis of $TiCl_4$, were immobilized onto Ch/PMA microparticles in order to evaluate their ability to photodegrade different textile azo dyes from aqueous solution: acid dyes C.I. Acid Orange 7, C.I. Acid Red 18, C.I. Acid Blue 113; reactive dyes C.I. Reactive Yellow 17, C.I. Reactive Black 5; and direct dye C.I. Direct Blue 78.

FTIR analysis showed that Ch and PMA were incorporated into the polymer network and presence of TiO_2 nanoparticles did not affect polymer network formation. The presence of Ti on the microparticles was confirmed by EDX analysis. SEM analysis and optical microscopy revealed that microparticles had spherical shape and approximate diameter of dry microparticles was 350 μm.

It was found that dyes C.I. Acid Blue 113 and C.I. Reactive Black 5 are prone to photolysis. Under illumination, blank microparticles showed poor sorption affinity toward all investigated dyes, except for C.I. Acid Blue 113. On the other hand, microparticles with immobilized colloidal TiO_2 nanoparticles successfully removed all dyes except C.I. Reactive Yellow 17 which was only 75% removed. It was found that pH played significant role in the degradation rate of dye C.I. Acid Orange 7. Reproducibility study was performed for the dye C.I. Acid Orange 7 at all investigated pH values and after three cycles of illumination removal degree was maintained at remarkably high level of more than 95%, indicating that fabricated microparticles could be reused without loss of photocatalytic efficiency.

Acknowledgements

The authors acknowledge funding from the Ministry of Education, Science and Technological Development of the Republic of Serbia, Project Nos. 172056 and 172062. The authors gratefully acknowledge Dr. Maja Vukašinović-Sekulić (University of Belgrade, Faculty of Technology and Metallurgy, Serbia) for her help in the optical microscopy, Dr. Slavica Lazarević (University of Belgrade, Faculty of Technology and Metallurgy, Serbia) for helping with BET isotherms and Andjelika Bjelajac (University of Belgrade, Faculty of Technology and Metallurgy, Serbia) for providing FE-SEM measurements.

References

[1] P.K. Dutta, J. Dutta, V.S. Tripathi, Chitin and chitosan: chemistry, properties and applications, J. Sci. Ind. Res. India 63 (1) (2004) 20–31.
[2] M. Rinaudo, Chitin and chitosan: properties and applications, Prog. Polym. Sci. 31 (7) (2006) 603–632.
[3] I.-Y. Kim, S.-J. Seo, H.-S. Moon, M.-K. Yoo, I.-Y. Park, B.-C. Kim, C.-S. Cho, Chitosan and its derivatives for tissue engineering applications, Biotechnol. Adv. 26 (1) (2008) 1–21.
[4] N. Mati-Baouche, P.-H. Elchinger, H. de Baynast, G. Pierre, C. Delattre, P. Michaud, Chitosan as an adhesive, Eur. Polym. J. 60 (2014) 198–212.
[5] A. Bornet, P.L. Teissedre, Applications and interest of chitin, chitosan and their derivatives in enology, J. Int. Sci. Vigne. Vin. 39 (4) (2005) 199–207.
[6] J.d. Santos Menegucci, M.-K.M.S. Santos, D.J.S. Dias, J.A. Chaker, M.H. Sousa, One-step synthesis of magnetic chitosan for controlled release of 5-hydroxytryptophan, J. Magn. Magn. Mater. 380 (2015) 117–124.
[7] Y. Cai, Y. Lapitsky, Formation and dissolution of chitosan/pyrophosphate nanoparticles: is the ionic crosslinking of chitosan reversible?, Colloid Surf B 115 (2014) 100–108.
[8] M.B. Dowling, R. Kumar, M.A. Keibler, J.R. Hess, G.V. Bochicchio, S.R. Raghavan, A self-assembling hydrophobically modified chitosan capable of reversible hemostatic action, Biomaterial 32 (13) (2011) 3351–3357.
[9] C. Butstraen, F. Salaün, Preparation of microcapsules by complex coacervation of gum Arabic and chitosan, Carbohyd. Polym. 99 (2014) 608–616.
[10] A.F. Martins, D.M. de Oliveira, A.G.B. Pereira, A.F. Rubira, E.C. Muniz, Chitosan/TPP microparticles obtained by microemulsion method applied in controlled release of heparin, Int. J. Biol. Macromol. 51 (5) (2012) 1127–1133.
[11] H. Omidian, M.J. Zohuriaan-Mehr, H. Bouhendi, Polymerization of sodium acrylate in inverse-suspension stabilized by sorbitan fatty esters, Eur. Polym. J. 39 (5) (2003) 1013–1018.
[12] A. Bernkop-Schnürch, S. Dünnhaupt, Chitosan-based drug delivery systems, Eur. J. Pharm. Biopharm. 81 (3) (2012) 463–469.

[13] M. Khosravi, S. Azizian, Adsorption of anionic dyes from aqueous solution by iron oxide nanospheres, J. Ind. Eng. Chem. 20 (4) (2014) 2561–2567.
[14] A.R. Khataee, M.B. Kasiri, Photocatalytic degradation of organic dyes in the presence of nanostructured titanium dioxide: influence of the chemical structure of dyes, J. Mol. Catal. A-Chem. 328 (1–2) (2010) 8–26.
[15] M.A. Henderson, A surface science perspective on TiO_2 photocatalysis, Surf. Sci. Rep. 66 (6–7) (2011) 185–297.
[16] M.A. Rauf, M.A. Meetani, S. Hisaindee, An overview on the photocatalytic degradation of azo dyes in the presence of TiO_2 doped with selective transition metals, Desalination 276 (1–3) (2011) 13–27.
[17] R.A. Damodar, T. Swaminathan, Performance evaluation of a continuous flow immobilized rotating tube photocatalytic reactor (IRTPR) immobilized with TiO_2 catalyst for azo dye degradation, Chem. Eng. J. 144 (2008) 59–66.
[18] S. Shoaebargh, A. Karimi, RSM modeling and optimization of glucose oxidase immobilization on TiO_2/polyurethane: feasibility study of AO7 decolorization, J. Environ. Chem. Eng. 2 (3) (2014) 1741–1747.
[19] L. Marija, M. Nedeljko, R. Maja, Š. Zoran, R. Marija, K.K. Melina, Photocatalytic degradation of C.I. Acid Orange 7 by TiO2 nanoparticles immobilized onto/into chitosan-based hydrogel, Polym. Compos. 35 (4) (2014) 806–815.
[20] M. Lučić, N. Milosavljević, M. Radetić, Z. Šaponjić, M. Radoičić, M. Kalagasidis Krušić, The potential application of TiO_2/hydrogel nanocomposite for removal of various textile azo dyes, Sep. Purif. Technol. 122 (2014) 206–216.
[21] D. Mihailovic, Z. Saponjic, M. Radoicic, T. Radetic, P. Jovancic, J. Nedeljkovic, M. Radetic, Functionalization of polyester fabrics with alginates and TiO_2 nanoparticles, Carbohyd. Polym. 79 (3) (2010) 526–532.
[22] T. Rajh, D.M. Tiede, M.C. Thurnauer, Surface modification of TiO_2 nanoparticles with bidentate ligands studied by EPR spectroscopy, J. Non-Cryst. Solids 205–207 (Part 2(0)) (1996) 815–820.
[23] R.C. Thompson, Oxidation of peroxotitanium(IV) by chlorine and cerium(IV) in acidic perchlorate solution, Inorg. Chem. 23 (13) (1984) 1794–1798.
[24] E.P. Barrett, L.G. Joyner, P.P. Halenda, The determination of pore volume and area distribution in porous substances. I. Computations from nitrogen isotherms, J. Am. Chem. Soc. 73 (1951) 373–380.
[25] Y. Boonsongrit, B.W. Mueller, A. Mitrevej, Characterization of drug-chitosan interaction by 1H NMR, FTIR and isothermal titration calorimetry, Eur. J. Pharm. Biopharm. 69 (1) (2008) 388–395.
[26] A. Pawlak, M. Mucha, Thermogravimetric and FTIR studies of chitosan blends, Thermochim. Acta 396 (1–2) (2003) 153–166.
[27] M.B.H. Othman, H. Md Akil, S.Z. Md Rasib, A. Khan, Z. Ahmad, Thermal properties and kinetic investigation of chitosan-PMAA based dual-responsive hydrogels, Ind. Crop. Prod. 66 (2015) 178–187.
[28] L. Huang, S. Yuan, L. Lv, G. Tan, B. Liang, S.O. Pehkonen, Poly(methacrylic acid)-grafted chitosan microspheres via surface-initiated ATRP for enhanced removal of Cd(II) ions from aqueous solution, J. Colloid Interface Sci. 405 (2013) 171–182.
[29] H.S. Mansur, A.A.P. Mansur, E. Curti, M.V. De Almeida, Functionalized-chitosan/quantum dot nano-hybrids for nanomedicine applications: towards biolabeling and biosorbing phosphate metabolites, J. Mater. Chem. B 1 (12) (2013) 1696–1711.
[30] G. Socrates, Infrared and Raman Characteristic Group Frequencies, third ed., John Wiley & Sons Ltd, England, 2001.
[31] W. Kangwansupamonkon, W. Jitbunpot, S. Kiatkamjornwong, Photocatalytic efficiency of TiO_2/poly[acrylamide-co-(acrylic acid)] composite for textile dye degradation, Polym. Degrad. Stabil. 95 (9) (2010) 1894–1902.
[32] C. Hou, Q. Zhang, Y. Li, H. Wang, P25–graphene hydrogels: room-temperature synthesis and application for removal of methylene blue from aqueous solution, J. Hazard. Mater. 205–206 (2012) 229–235.
[33] G.G. Maghami, G.A.F. Roberts, Studies on the adsorption of anionic dyes on chitosan, Die Makromol. Chem. 189 (10) (1988) 2239–2243.
[34] B.D. Gummow, G.A.F. Roberts, Studies on chitosan-induced metachromasy, 1. Metachromatic behaviour of sodium 2′-hydroxy-1,1′-azonaphthalene-4-sulfonate in the presence of chitosan, Die Makromol. Chem. 186 (6) (1985) 1239–1244.
[35] C.H. Giles, A.S.A. Hassan, R.V.R. Subramanian, Adsorption at organic surfaces IV—adsorption of sulphonated azo dyes by chitin from aqueous solution, J. Soc. Dyer. Colourist. 74 (10) (1958) 682–688.
[36] P.O. Osifo, A. Webster, H. van der Merwe, H.W.J.P. Neomagus, M.A. van der Gun, D.M. Grant, The influence of the degree of cross-linking on the adsorption properties of chitosan beads, Bioresour. Technol. 99 (15) (2008) 7377–7382.
[37] M.R. Hoffmann, S.T. Martin, W. Choi, D.W. Bahnemann, Environmental applications of semiconductor photocatalysis, Chem. Rev. 95 (1) (1995) 69–96.
[38] J. Saien, A.R. Soleymani, Degradation and mineralization of Direct Blue 71 in a circulating upflow reactor by UV/TiO_2 process and employing a new method in kinetic study, J. Hazard. Mater. 144 (1–2) (2007) 506–512.
[39] R.B.M. Bergamini, E.B. Azevedo, L.R.R. de Araujo, Heterogeneous photocatalytic degradation of reactive dyes in aqueous TiO_2 suspensions: decolorization kinetics, Chem. Eng. J. 149 (1–3) (2009) 215–220.
[40] Z. Bouberka, K.A. Benabbou, A. Khenifi, U. Maschke, Degradation by irradiation of an Acid Orange 7 on colloidal TiO_2/(LDHs), J. Photochem. Photobiol. A: Chem. 275 (2014) 21–29.
[41] Y.-n. Liu, H. Xu, S.-F. Zhu, M. Zhou, J. Miao, Enhanced degradation of acid orange 7 solution by non-thermal plasma discharge with TiO_2, Plasma. Chem. Plasma. Process. 34 (6) (2014) 1403–1413.
[42] I.K. Konstantinou, T.A. Albanis, TiO_2-assisted photocatalytic degradation of azo dyes in aqueous solution: kinetic and mechanistic investigations – a review, Appl. Catal. B-Environ. 49 (1) (2004) 1–14.